Chapter 12

Analysis of a Coextrusion Process for Preparing Gradient-Index Polymer Optical Fibers

Yung Chang, Wen-Chang Chen*, Ming-Hsin Wei, and Wen-Chung Wu

Department of Chemical Engineering, National Taiwan University, Taipei, Taiwan 106, Republic of China

A theoretical modeling was introduced on a coextrusion process for preparing gradient-index (GI) polymer optical fibers (POFs). The effects of the mass transfer coefficient (k) between the fiber preform and the purging gas, and the interlayer number (n) on the refractive index distribution (RID) of POFs were investigated. The predicted refractive index distribution (RID) was in a satisfactory agreement with the experimental data reported in the literature. The order of Δn value in the studied systems was $k^*(\sim \infty) > k^* (=5) > k^* (\sim 0)$ for various interlayer numbers. As k closes to a very small or a very large value, the RID deviates significantly from the parabolic RI distribution. The order of the degree of the RI distribution close to a parabolic distribution is five-layer > four-layer > three-layer > two-layer. The result suggests that the greater the layer number in the multilayer coextrusion process, the closer the RID is to a parabolic curve. These results provide a way to monitor the RID of POFs by process design.

Scientific interest in gradient-index (GI) polymer optical fibers (POFs) remains very high in light of their versatile applications in optical communication, imaging, and collimating (*1-6*). New types of high transmission speed of POFs for communication

1: corresponding author

In Optical Polymers; Harmon, Julie P., et al.;
ACS Symposium Series; American Chemical Society: Washington, DC, 2001.

applications have been reported recently. Giaretta et al. developed a GI POF based on perfluorinated (PF) polymer with a transmission speed as high as 11 Gb/s at 1.3 μm (*7*). A theoretical study on the attenuation limit of PF GI polymer optical fiber (POF) was estimated to be as low as 0.3 dB/km, which is comparable to that of a silica fiber in the near infrared region (*1*). Koike and his coworkers demonstrated that GI POF can be used as an optical fiber amplifier by doping the fiber with organic dyes (*8*). Another potential application of GI Polymers is as the essential components of the selfoc lens array (SLA) in fax machines and scanners (*9,10*).

The refractive index variation inside the GI POF is described by the following two equations:

$$n(r) = n_1\left[1 - 2\delta\left(\frac{r}{R}\right)^g\right]^{\frac{1}{2}} \qquad 0 \le r \le R \tag{1}$$

$$\delta = \frac{n_1 - n_2}{n_1} \tag{2}$$

Where n_1 and n_2 are the refractive indices of the center axis and the periphery, respectively, R is the fiber radius, and g is the index exponent of the power law. It was found that the bandwidth of a GI POF is maximized when g has the value of 2 (*11*). That is, the optimal RID is a parabolic curve. Koike et al demonstrated the importance of materials dispersion on the bandwidth of GI POF. They concluded that the g values must be in the range of 1.70-3.0 for achieving high transmission speed (> 1 Gb/s) using a light source with more than 2-nm spectral width (*12*). For the GI lens applications, keeping both Δn greater than 0.01 and $g \cong 2$ are very important for the imaging applications (*9,10*). Hence, optimization of the refractive index distribution to a quadratic distribution is very important for GI POF.

In order to achieve a parabolic RID for a POF, both materials system and process design are required to be considered. The differences between the monomer concentration, monomer reactivity, monomer size, monomer density, monomer diffusivity, the properties of the host polymers, and external process design were the driving forces behind producing index gradients inside the fiber. Multilayer coextrusion has been recognized as a potential method for preparing GI POFs. Diffusion of various monomers through each layer and the mass transfer between the fiber preform and the purging nitrogen results in a distribution of refractive index inside the fiber. Based on the purging nitrogen condition on the diffusion zone, it can be classified as the closed process (k =0) and open process (k >0). Our laboratory has done extensive experimental (*13-15*) and theoretical work (*16-18*) on a multilayer coextrusion process for preparing GI POF. Furthermore, a general theoretical modeling of the N-layer coextrusion process was developed to predict the effects of the essential parameters on the RID of POF (*18*). However, the effects of the k values for the high interlayer numbers (four or five layer) on RID of POFs for both the closed and open processes have not been fully explored in the previous study (*18*).

In this study, an extended work on the theoretical analysis of the multilayer coextrusion process for preparing GI POFs is reported. The effects of the mass

transfer coefficient (k) between the fiber preform and the purging nitrogen, and the layer number (n) on the refractive index distribution (RID) of POFs were investigated. The theoretical prediction was compared with the experimental results by us (*13*) and Toyoda et al (*10*). The basic parameters for the present mathematical simulation are shown in Table 1. The effects of the k values on the RID of POFs and the two-five layer coextrusion process were examined.

Coextrusion Process for Preparing GI POF

A similar essential design of the N-layer coextrusion process has been described previously (*18*) and briefly shown here. Figure 1 shows the schematic diagram of the apparatus of the N-layer closed (no nitrogen purging) and open (nitrogen purging) coextrusion process for preparing GI POF. Material tanks (**1~N**) containing a solution of a polymer and monomers were heated at a desired temperature (e.g., 60^0C). Next, the polymer solutions in the tanks (**1~N**) were fed by the gear pumps ($\mathbf{G_1}$~$\mathbf{G_N}$) to the concentric die (**D**). Here, the refractive indices of the polymer solutions inside the concentric die were arranged in the order of decreasing from the center to the periphery of the die. The order of the refractive index in the N sections is $N_1 > N_2 > N_3 >$ -------- $>N_{N-1}> N_N$. The volume ratios of the polymer solutions from different tanks can be adjusted to obtain the desired refractive index distribution. A N-layer composite monofilament was then extruded out of the orifice of the die and fed into a diffusion zone (**Z**) with a length of L. While the monofilament went through the diffusion zone, the monomer in each layer diffused into each other to produce the refractive index distribution. In the closed extrusion process (a: k=0), the diffusion zone was insulated from the surrounding. In the open process (b:k>0), a hot nitrogen gas was purged through the diffusion zone and thus the mass transfer occurred between the fiber and its periphery. The monofilament was then fed through a hardening zone (**H**) where it was hardened by UV lamps. A polymer fiber with a certain RID was taken up through rolls by a take-up roll (**I**).

Theoretical Analysis

A theoretical modeling based on the above process has been derived previously (18). Briefly, the governing equations and the composition distribution are shown here. Let r and z are the radial distance and the distance measured from the top of the diffusion zone, respectively. R and L are the radius and the length of the diffusion zone. The variation of the mass fraction of monomer M, x, inside the diffusion zone at a steady-state operation can be described by

$$u\frac{\partial x}{\partial z} = D_r\left(\frac{\partial^2 x}{\partial r^2} + \frac{1}{r}\frac{\partial x}{\partial r}\right) + D_z\frac{\partial^2 x}{\partial z^2} \qquad (3)$$

Table I. Experimental Conditions[a] Used in the coextrusion process(*10,13*).

Item	*Two-layer*	*three-layer*	*Four-layer*	*five-layer*
		Mixture 1 (inner layer)		
PMMA(%)	58	52	52	52
BzMA(%)	28	35	35	35
MMA(%)	14	13	13	13
		Mixture 2 (second layer)		
PMMA(%)	60	50	50	50
BzMA(%)	0	15	15	15
MMA(%)	40	35	35	35
		Mixture 3 (third layer)		
PMMA(%)	-	50	50	50
BzMA(%)	-	-	-	-
MMA(%)	-	50	50	50
		Mixture 4 (fourth layer)		
PMMA(%)	-	-	47	47
BzMA(%)	-	-	-	-
MMA(%)	-	-	40	40
FPMA(%)	-	-	13	13
		Mixture 5 (outer layer)		
PMMA(%)	-	-	-	40
BzMA(%)	-	-	-	-
MMA(%)	-	-	-	18
FPMA(%)	-	-	-	42
R(mm)	0.5	0.59	0.6	0.6
u (cm/min)	254	40	40	40
T(°C)	80	60	60	60
L(cm)	45	45	45	45
Radius ratio(2-layer)	$0.5(R^*_{f1}):1(R^*_{f2})$			
Radius ratio(3-layer)	$0.76(R^*_{f1}):0.96(R^*_{f2}):1(R^*_{f3})$			
Radius ratio(4-layer)	$0.75(R^*_{f1}):0.94(R^*_{f2}):0.98(R^*_{f3}):1(R^*_{f4})$			
Radius ratio(5-layer)	$0.73(R^*_{f1}):0.92(R^*_{f2}):0.96(R^*_{f3}):0.98(R^*_{f4}):1(R^*_{f5})$			

[a]The RI values of PMMA, Poly(BzMA), and Poly(FPMA) used in the present study are 1.490(*21*), 1.568(*21*), and 1.425(*22*), respectively. The densities of PMMA, Poly(BzMA), Poly(FPMA) used in the present study are 1.170(*21*), 1.179(*21*), and 1.496(*22*), respectively.

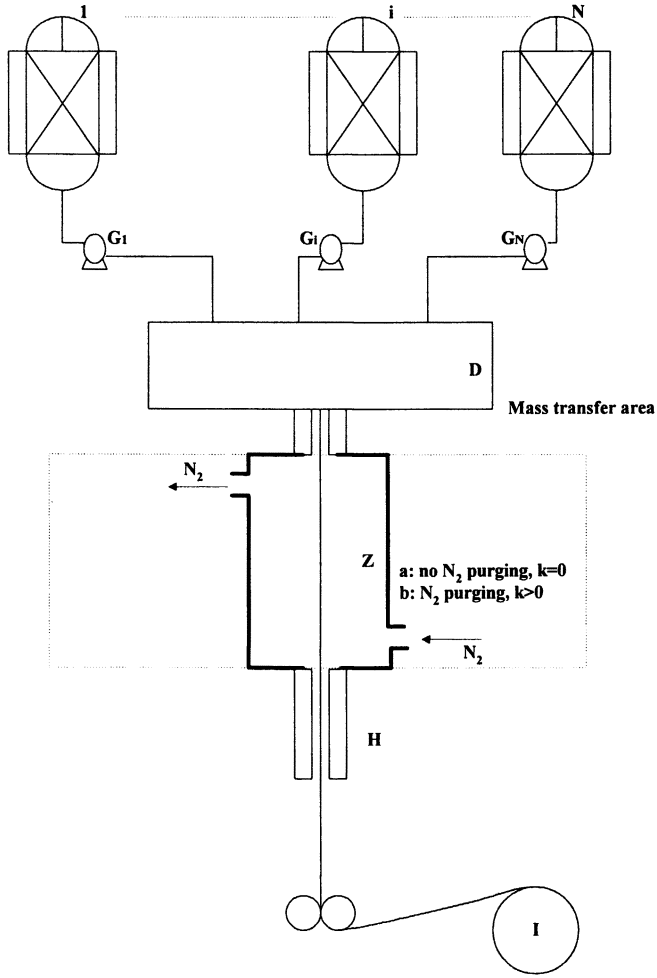

Figure 1. Schematic representation of a N-layer coextrusion process.1,...,i,...N , material supply tanks; $G_1,...,G_i,...G_N$, gear pumps; D, a concentric die; Z, diffusion zone (a: no N2 purging, b: N2 purging); H, a hardening zone; I, rolls.

where u denotes the extrusion velocity, and D_r and D_z the effective diffusivities of monomers in the r and z directions respectively. The boundary conditions associated with equation (3) are summed as follows :

$$x \text{ is finite at } r = 0 \tag{4a}$$

$$-D_r \frac{\partial x}{\partial r} = kx \text{ at } r = R \tag{4b}$$

where k represents the mass transfer coefficient of monomer, M, between the fiber periphery and the purged nitrogen. For the importance of practical applications, the peclect number (uL/D_z) is large, i.e., the transport of the monomers due to convection motion is more significant than that due to molecular diffusion. Therefore, the last term of equation (3) is much smaller than the term on the left-hand side. In this case, equation (3) can be solved in the following dimensionless mass fraction of monomer M at the outlet of the diffusion zone (z=L),

$$x_M^* = 2\sum_{m=1}^{\infty} \left[\frac{k^* x_{M,N}^* J_0(\lambda_m) + \sum_{i=2}^{N} (x_{M,i-1}^* - x_{M,i}^*) \lambda_m R_{f_{i-1}}^* J_1(\lambda_m R_{f_{i-1}}^*)}{J_0^2(\lambda_m)(k^{*2} + \lambda_m^2)} \right] \times \exp\left(-\lambda_m^2 z_M^*\right) J_0\left(\lambda_m r^*\right) \tag{5}$$

In this expression, $r^* = r/R$, J_0 and J_1 are the Bessel functions of the first kind of orders 0 and 1 respectively, λ_m is the positive root of $k^* J_0(\lambda_m) = \lambda_m J_1(\lambda_m)$. And

$$x_M^* = x_M / x_{M,0} \tag{6a}$$

where x_M is the mass fraction of monomer M in the the diffusion zone at z and $x_{M,0}$ is the largest mass fraction of the monomer M in the multi-layer at z=0. And

$$z_M^* = \frac{zD_r}{uR^2} \tag{6b}$$

$$k^* = \frac{kR}{D_r} \tag{6c}$$

Extreme cases. Two extreme cases can be recovered directly from the present model : k* is very small (k*→0),and k* is very large (k*→∞). The special case of k*→0 corresponds to a closed co-extrusion. That means there is no mass transfer between the fiber periphery and the purged gas. In this case, equation (5) reduce to equation (7).

$$x_M^* = x_{M,N}^* + \sum_{i=2}^{N}(x_{M,i-1}^* - x_{M,i}^*)R_{f_{i-1}}^{*2} + 2\sum_{m=1}^{\infty}\left[\frac{\sum_{i=2}^{N}(x_{M,i-1}^* - x_{M,i}^*)R_{f_{i-1}}^* J_1(\lambda_m R_{f_{i-1}}^*)}{\lambda_m J_0^2(\lambda_m)}\right] \times \exp(-\lambda_m^2 z_M^*) J_0(\lambda_m r^*) \quad (7)$$

where λ_m is the positive root of $J_1(\lambda_m)=0$. The other extreme, $k^* \to \infty$, implies that a perfect permeability at the outer boundary of the diffusion zone. In this case, equation (5) reduce to equation (8).

$$x_M^* = 2\sum_{m=1}^{\infty}\left[\frac{x_{M,N}^*\lambda_m J_1(\lambda_m) + \sum_{i=2}^{N}(x_{M,i-1}^* - x_{M,i}^*)\lambda_m R_{f_{i-1}}^* J_1(\lambda_m R_{f_{i-1}}^*)}{\lambda_m^2 J_1^2(\lambda_m)}\right] \times \exp\left(-\lambda_m^2 z_M^*\right) J_0\left(\lambda_m r^*\right) \quad (8)$$

where λ_m is the positive root of $J_0(\lambda_m)=0$.

The transformation of the fiber composition to refractive index distribution can be performed as below. Lorentz and Lorenz (28,29) suggested that the optical property of a non-absorbing media and its chemical structure correlate through an additive rule. The refractive index of a composite material, for example, can be represented by equation (9), (30).

$$n_d = \sqrt{\frac{1+2\phi}{1-\phi}} \quad (9)$$

with

$$\phi = \frac{\sum_M \frac{n_{d,M}^2 - 1}{n_{d,M}^2 + 2}\frac{x_M}{\rho_M}}{\sum_M \frac{x_M}{\rho_M}} \quad (9a)$$

where $n_{d,M}$ and ρ_M are the refractive index and density of the component M. Therefore, the refractive index of the GI POF by the N-layer extrusion process can be determined by the combination of equation (5) and equation (9). The index exponent (g) of the RI distribution can be obtained by fitting the predicted data with equation (1). Furthermore, the difference between the fiber center and periphery (Δn) can be determined by the difference of the fiber center (n_1) and the periphery (n_2)

Results and Discussion

The present model is justified with the experimental data obtained from the two-layer closed coextrusion process by Ho et al. (*13*) and the three-five layer open coextrusion processes by Toyoda.(*10*). The experimental parameters of these processes are shown in Table 1.

Two-layer Closed Process. Figure 2 shows the variation of RI of a fiber n as a function of its dimensionless radius, r* at various k* values for the two-layer coextrusion process. The case of k* = 0 is the closed process while the other two k* values are the open process. The predicted result at k*=0 by the present model is in satisfactory agreement with the experimental result by Ho et al. (13). The estimated values of Δn and g for k* =0, 5, and ∞ are 0.0178 and 0.95, 0.0179 and 0.96, 0.031 and 1.00, respectively. This result suggests that the Δn value enhances and the RID gets close to a parabolic distribution with increasing the k* value. The case of k*=0 implies that k=0 from equation (6c) (for a fixed diffusion coefficient D_r). That is, there is no mass transfer between the fiber preform and the periphery. Once the k* value increases, the mass transfer between the fiber preform and the purging nitrogen increases. That is, the low refractive index monomer MMA evaporating from the fiber preform results in increasing the refractive index difference between the fiber center and periphery. This explains the variation of the RID with various k* values shown in figure 2. Although the g value increases from 0.95 to 1.00 as k* increases from 0 to ∞, it is still far away from a parabolic distribution (g =2). There are several approaches to improve the RID of the two-layer coextrusion process: (1) select different polymer/monomer mixture; (2) use a core- shell separation process to cut out the non-parabolic fiber preform after passing through the diffusion zone; and (3) use a higher layer number. From the theoretical estimation, the g values in the range of r* of 0-0.5 shown in figure 2 are1.41, 1.79 and 1.81 for the k* value of 0, 5, and ∞, respectively. Hence, the parabolic distribution of GI POFs can be possibly obtained by the core-shell separation design assisted with the theoretical study for the two-layer coextrusion process. An experimental design based on the core-shell separation design has been successfully developed for preparing the GI POFs with a parabolic distribution (14).

Three ~ Five layer IDSE Coextrusion Processes. The three-layer coextrusion process has been extensively studied previously (18). The estimated values of Δn and g in the present study for k* =0, 5, and ∞ are 0.003, 1.01, 0.013 and 2.13, 0.030 and 1.58, respectively. The Δn value is enhanced and the g value gets closer to 2 compared the two-layer coextrusion process shown in the previous section. This result suggests that the addition of a third-layer with a proper selection of polymer mixture can improve the index gradient over the two-layer case. However, the g value deviates from the parabolic distribution as k* increases from 5 to ∞. This result indicates that an optimum k* value is required to obtain a parabolic RID. Note that the only monomer present in the outmost layer is MMA as shown in Table 1, with a relatively low RI. Hence, if the mass transfer is too large between the fiber preform and purging

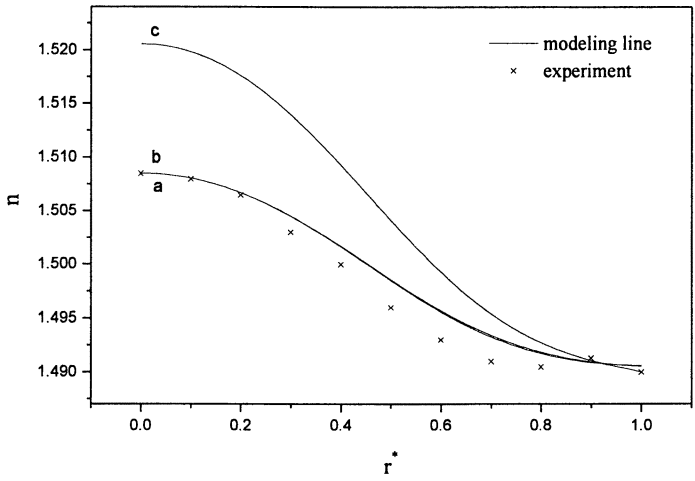

Figure 2. Variation of RI of a fiber n as a function of its dimensionless radius, r^*. at various k^*. Curve a, $k^* \rightarrow 0$; curve b, $k^*=5$; curve c, $k^* \rightarrow \infty$. The experimental conditions are shown in column 1 of Table 1. Parameters used are $z^*_{BzMA}=0.03$, $z^*_{MMA}=0.03$, $R^*_{f1}=0.5$.

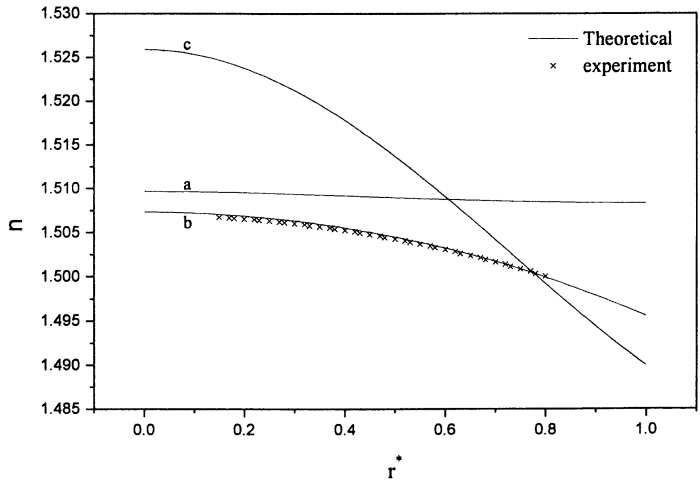

Figure 3. Variation of RI of a fiber n as a function of its dimensionless radius, r^*. at various k^*. Curve a, $k^* \rightarrow 0$; curve b, $k^*=5$; curve c, $k^* \rightarrow \infty$. The experimental conditions are shown in column 3 of Table 1. Parameters used are $z^*_{BzMA}=0.215$, $z^*_{MMA}=0.215$, $R^*_{f1}=0.75$, $R^*_{f2}=0.94$, $R^*_{f3}=0.98$.

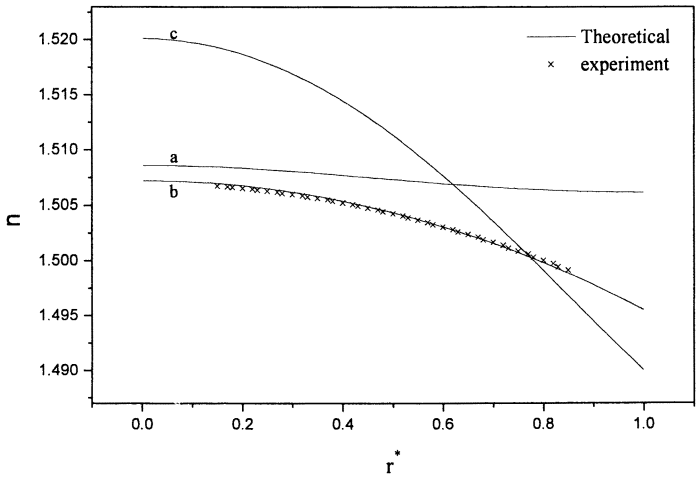

Figure 4. Variation of RI of a fiber n as a function of its dimensionless radius, r^*. at various k^*. Curve a, $k^* \rightarrow 0$; curve b, $k^*=5$; curve c, $k^* \rightarrow \infty$. The experimental conditions are shown in column 4 of Table 1. Parameters used are $z^*_{BzMA}=0.2$, $z^*_{MMA}=0.2$, $R^*_{f1}=0.73$, $R^*_{f2}=0.92$, $R^*_{f3}=0.96$, $R^*_{f4}=0.98$.

nitrogen, most of the MMA monomer is driven out of the fiber preform but the monomer BzMA with a high boiling point remains. Hence, the g value decreases if k* increases from 5 to ∞.

Figures 3 and 4 show the variation of RI of a fiber n as a function of its dimensionless radius, r* at various k* values for the four and five-layer coextrusion processes, respectively. As presented in the previous publication (*18*), the predicted results by the present model (at k*=5) are in a satisfactory agreement with the experimental data of Toyoda (15). Here, a further study on the extreme cases (k*→0 and k*→∞) is presented. The estimated values of Δn and g in the four-layer case for k* =0, 5, and ∞ are 0.001 and 1.01, 0.012 and 2.07, 0.036 and 1.55, respectively. For the case of the five-layer case, the Δn and g values for k* =0, 5, and ∞ are 0.002 and 1.01, 0.012 and 2.04, 0.030 and 1.76, respectively. Similar to the three-layer case, as k* closes to a very small or a very large, the RID deviates significantly from the parabolic RI distribution. The g values in the case of k*=5 for the two-five layer coextrusion process are 0.96, 2.13, 2.07, and 2.04, respectively. That is, the more the number of layers, the closer the RID is to a parabolic curve if the proper polymer mixture of each layer is selected. This is because the refractive index gradient of polymer mixture in each layer is easily adjusted as the layer number increases.

Conclusions

A theoretical modeling was successfully developed to predict the multilayer coextrusion process for preparing GI POFs. The order of Δn value increases as the value of mass transfer coefficient (k) increases. As k* becomes very small or very large, the RID deviates significantly from the parabolic RI distribution. The order of the degree of the RI distribution close to a parabolic distribution is five-layer > four-layer > three-layer > two-layer. The result suggests that the greater the layer number in the multilayer coextrusion process, the closer the RID is to a parabolic curve if the proper polymer composition in each layer is selected. These results provide a way to monitor the RID of GI POFs by process design.

References

1. Koike, Y., Ed. Proceeding of Seventh International Conference on Plastic Optical Fibers and Applications, Berlin, October 5-8, **1998**.
2. Kaino, T. in Polymers for Lightwave and Integrated Optics, edited by L. A. Hornak (Marcel Dekker, Inc.: New York, **1992**), Chapter 1.
3. Koike, Y.; Nihei, R. U. S. Patent, 5,593,621, **1997**.
4. Blyler, Jr., L. L., in Ref.1 ,**1998**, A1-A5.
5. Quan, X. Polymer Preprints **1999**, 39, 1279.
6. Garito, A. F.; Wang, J.; Gao, R. Science **1998**, 281, 962.
7. Giaretta, G.; White, W.; Wegmueller, M.; Yelamarty, R. V.; Onishi, T. Proc. OFC/IOOC'99 **1999**, postdeadline papers, PD14-1.
8. A. Tayaga, T. Kobayashi, S. Nakatsuka, E. Nihei, K. Sasaki, and Y. Koike, Jpn. J. Appl. Phys.**1997**, 36, 2705.
9. Yamamoto, T.; Mishina, Y.; Oda, M. U. S. Patent, 4,582,982, **1989**.
10. Toyoda, N.; Mishina, Y.; Murata, R.; Uozu, Y.; Oda, M.; Ishimaru, T. U. S. Patent, 5,390,274, 1995.
12. Ishigure, T.; Nihei, E.; and Koike, Y., Polymer J. **1996**, 28, 272.
13. Ho. B. C.: Chen, J. H.; Chen, W. C.; Yang, S. Y.; Chen, J. J.; Tseng, T. W. Polymer J. **1995**, 27, 310.
14. Chen, W. C. Chen, J. H.; Yang, S. Y.; Cherng, J. Y.; Chang, Y. H.; Ho, B. C. J. Appl. Polym. Sci. **1996**, 60, 1379.
15. Chen, W. C. ; Chen, J. H.; Yang, S. Y.; Chen, J. J.; Chang, Y. H.; Ho, B. C.; Tseng, T. W. ACS Symp. Ser. **1997**, 672, 71.
16. Liu, B.-T.; Chen, W. C.; Hsu, J.-P. Polymer **1999**, 40, 1451.
17. Liu, B.-T.; Hsieh, M.-Y.; Chen,W. C.; Hsu, J.-P.; Polymer J. **1999**, 31 ,233.
18. Chen, W. C.; Chang, Y.; Hsu, J. P, J. Phys. Chem. B **1999**, 103, 7584.
19. Lorentz, H. A. Wied. Ann. Phys. **1880**, 9, 641.
20. Lorenz, L. V.; Wied. Ann. Phys. **1880**, 11, 70.
21. Van Krevelen, D. W. Properties of Polymers, 3rd ed., Elsevier: Amsterdam, The Netherlands, **1990**; Chapters 4 and 10.
22. Tsai, C. C. Ph.D. thesis, National Tsing-Hua University, Hsinchu, Taiwan, 1995.